Diffusion Combustion in a Tube-Nested Combustor*

Tetsuji SEKO**, Ryosuke MATSUMOTO**, Yoshitomo SHINTANI**, Isao ISHIHARA** and Mamoru OZAWA**

An advanced-type compact water-tube boiler has been designed on the basis of the new concept of cooling flame by water-tube bank in the furnace, and is referred to as "tube-nested combustor". It realized drastic reduction in boiler size as well as in the NO_x emission. In this present study, aiming at further improvement of boiler efficiency and reduction of NO_x emission, the combustion characteristics in the furnace were investigated by using the test boiler of 0.5 t/h steam output. Experimental results indicated that the NO_x formation was restricted in the narrow area close to the burner exit, and that the CO-concentration decreased drastically with the combustion gas stream through the tube-bank. These facts were closely related to the experimental evidence of the cross-sectional distribution of gas temperature being rather uniform owing to the agitation by the tube-bank. These experimental results verified the soundness of the boiler design and, in addition, gave relevant information on local combustion characteristics available for the R&D of the next generation tube-nested combustor.

Key Words: Tube-Nested Combustor, Low NO_x Emission, Diffusion Combustion, Combustion Characteristics

1. Introduction

Increasing attention has been given to the global environmental problem. In the field of compact boilers, technological development for the reduction of emissions, e.g. CO_2, NO_x, and for the improvement of boiler efficiency is indispensable.

The advanced-type compact water-tube boiler shown in Fig. 1, being referred to as "tube-nested combustor", was developed by Ishigai et al.[1] and Ueda et al.[2], and has been well acknowledged by the market so far[3]. This type of boiler was designed on the basis of the new concept, being referred to as the JAFI(R) (JAggy FIreball) concept: suitably designed water-tube bank is placed closely to the burner, so that the conventional empty furnace is, in principle, removed. This concept realized drastic reduction in boiler size as well as in the NO_x emission. However, only limited information on the local combustion characteristics of the tube-nested combustor has been so far obtained, i.e., the detailed distribution of gas temperature and gas concentrations is an essential data to be obtained for further development of this technology. Thus, in this present study, aiming at the design basis for the next-generation tube-nested combustor, the local combustion characteristics were measured by using JAFI test boiler of 0.5 t/h steam output.

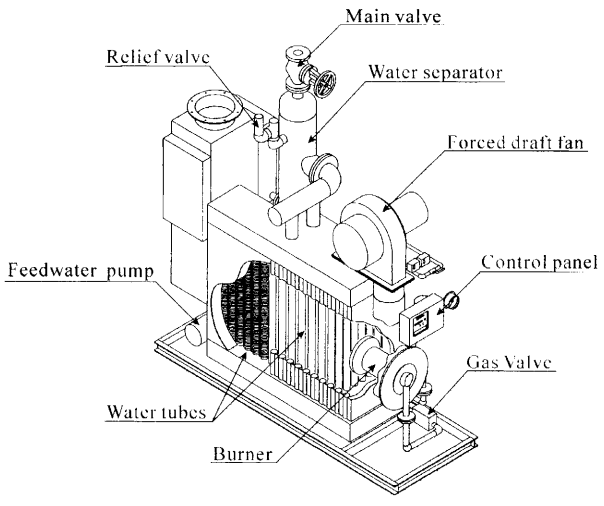

Fig. 1 Tube-nested combustor

* Received 30th July, 2003 (No. 03-4174)

** Department of Mechanical Engineering, Kansai University, 3–3–35 Yamate-cho, Suita, Osaka 564–8680, Japan. E-mail: matumoto@kansai-u.ac.jp

2. Experiment

The 0.5 t/h test boiler is shown in Fig. 2, and the specifications are summarized in Table 1. Table 1 also lists the fuel used in this experiment and experimental conditions. The test boiler consists mainly of a diffusion burner, a steam-generating water-tube bank, and a water circulation system. The diffusion burner is installed at the position 120 mm lower from the middle height of the furnace. The combustion gas issuing from the burner passed through the tube-bank being placed closely to the burner, and flowed into the exhaust duct. The tube-bank consists of bare and finned tubes as designated in Fig. 2, where the former agitates the impinging flame so as to promote combustion and cooling the flame, and the latter enhances the heat absorption by extended heating surfaces. In the part of bare tubes surrounded by even high temperature gas, the convective heat transfer exerts considerable influence on the heat absorption rate owing to the high velocity and enhanced mixing of gas in the tube-bank. In the present test boiler, the cross-sectional area of the combustor is reduced at the downstream so as to adjust the steam output. As shown in Table 1, the water-tubes with an outer diameter D_o of 50.8 mm and 800 mm height are arranged in the in-line array with longitudinal pitch $L/D_o = 1.97$, and transverse pitch $H/D_o = 1.57$, where H and L represent the transverse and longitudinal center-to-center distances of tubes, respectively. As shown in Fig. 2, eleven gas sampling taps are installed on the sidewall of the boiler at the middle height of the furnace and at the positions 200 mm higher/lower from there as shown in Fig. 2.

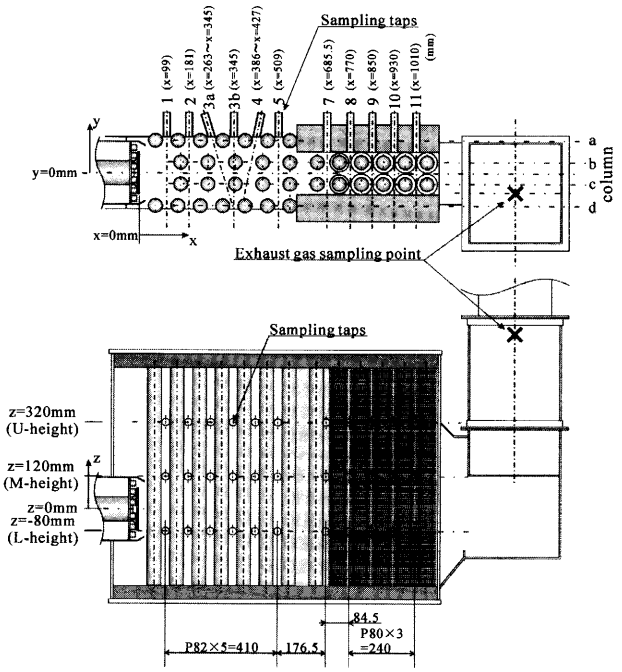

Fig. 2 Cross-section of test boiler

Table 1 Characteristics of the test boiler

Outer diameter of tube [mm]	D_o	50.8
Inner diameter of tube [mm]	D_i	44.4
Length of tube [mm]	l	800
Longitudinal pitch [-]	L/D_o	1.97
Transversal pitch [-]	H/D_o	1.57
Fuel		city gas 13A
Fuel gas flow rate [m^3/h]		32
Air ratio [-]	γ	1.5
Steam pressure [kPa]		700

In this investigation, two series of experiments were conducted. First, gas temperature distribution in the tube-bank was measured by R-type thermocouple supported within an insulation tube or by K-type sheathed thermocouple. The second series of experiments analyzed CO, NO_x and O_2 concentrations by non-dispersive infrared absorption, cross modulation chemiluminescence, and zirconia method, respectively, in the tube-bank. In both of the experiments, the thermocouple and the gas sampling probe were inserted through the gas sampling tap, and was traversed every 10 mm from $y = 0$ mm to $y = \pm 120$ mm or $y = \pm 70$ mm along dashed lines designated in the horizontal cross-section shown in Fig. 2. In addition to these measurements, gas temperature and gas concentrations were measured at the exhaust duct. The local temperature and gas concentrations presented in this paper are averaged values of 36 sampled data during 180 sec.

3. Exhaust Gas Characteristics

The NO_x reduction by the flame cooling is always accompanied by the problem of excess-cooling by the flame quenching resulting in an increase in the unburned CO emission.

The exhaust gas temperature and gas concentrations are shown in Table 2 where the NO_x-concentration was converted by $(NO_x \cdot 21)/21$ to the corresponding value at 0% O_2, being referred to as the reduced concentration. The reduced NO_x-concentration was at low level enough to meet the environmental regulation, although any alternative means, e.g. the pre-mixed burner or the exhaust gas recirculation effective for reducing NO_x emission, were not employed. The CO-concentration was also at low level of about 55 ppm. These facts verified the soundness of the design principles based on the JAFI concept.

4. Gas Temperature and Gas Concentrations

The distribution of gas temperature, the reduced NO_x-concentration, CO- and O_2-concentration at each height is shown, respectively, in Figs. 3 to 5. The heights of the

Table 2 Characteristics of exhaust gas

NO_X (at 0% O_2) [ppm]	CO [ppm]	O_2 [%]	Temperature [K]
43.4	53.9	8.0	594.2

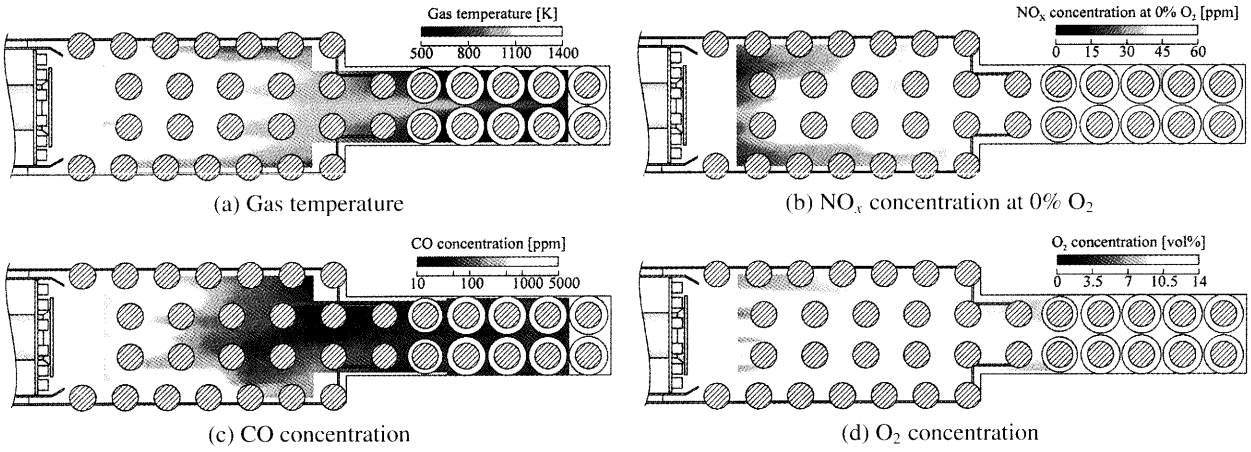

(a) Gas temperature (b) NO_x concentration at 0% O_2

(c) CO concentration (d) O_2 concentration

Fig. 3 Distribution of gas temperature and gas concentrations at L-height

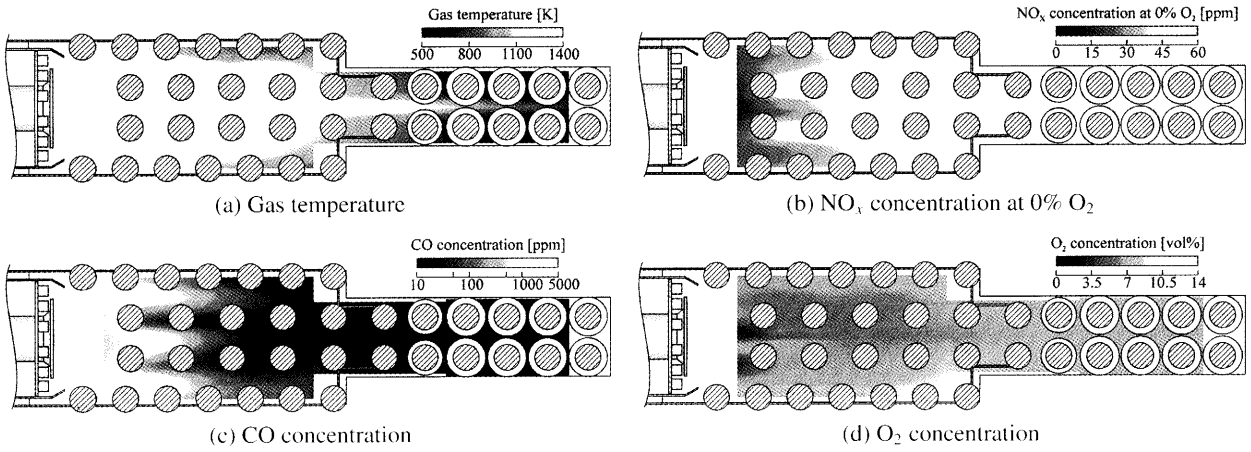

(a) Gas temperature (b) NO_x concentration at 0% O_2

(c) CO concentration (d) O_2 concentration

Fig. 4 Distribution of gas temperature and gas concentrations at M-height

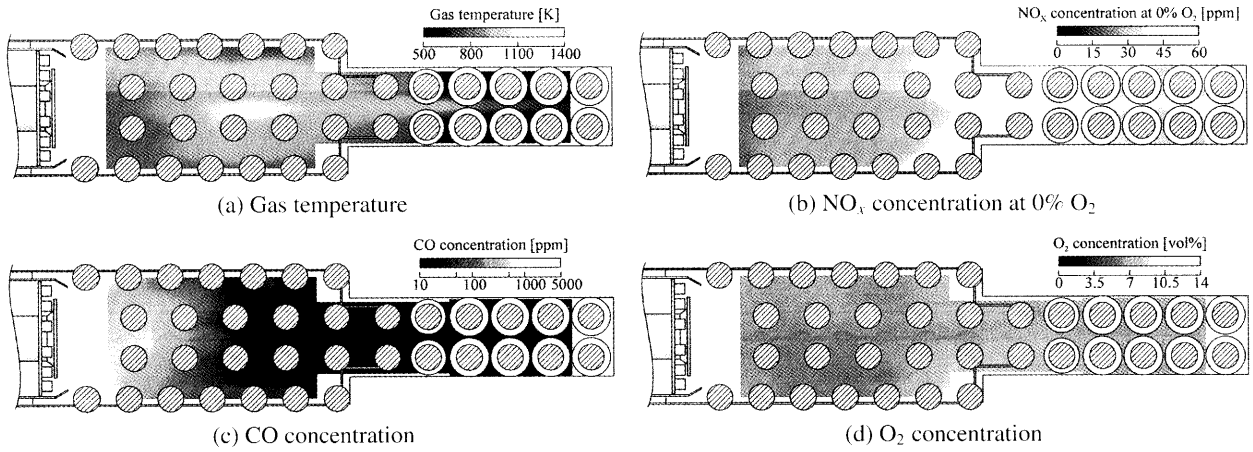

(a) Gas temperature (b) NO_x concentration at 0% O_2

(c) CO concentration (d) O_2 concentration

Fig. 5 Distribution of gas temperature and gas concentrations at U-height

measurement points relative to the burner location are illustrated in Fig. 6.

First, the measured data on the (1)-line, designated in Fig. 2, near the burner are explained. The temperature distributions at the L-height and M-height (also see Fig. 2) shown in Figs. 3 and 4 indicate relatively large fluctuations in the transverse distribution. This may be due to the flame formation by the baffle nozzle of the burner. The O_2-concentration shows a negative correlation to the gas temperature distribution. The CO-concentration is very high exceeding 5 000 ppm in the burner exit region. This indicates existence of intense combustion reaction there. The NO_x-concentration shows similar tendency to the temperature distribution. This is a typical evidence that the tem-

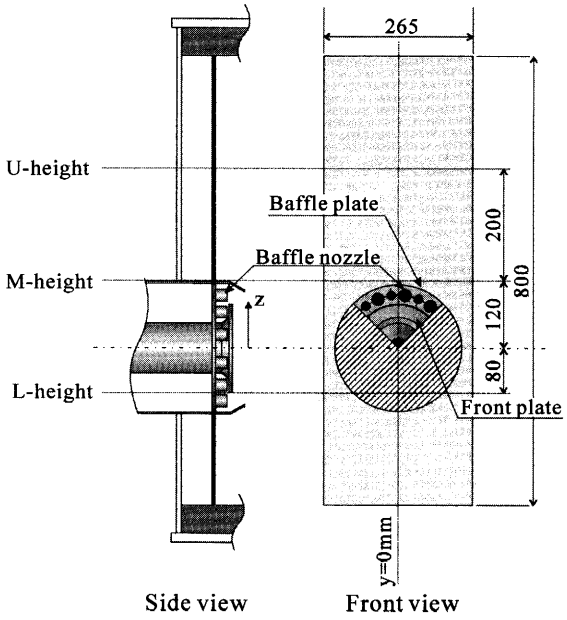

Fig. 6 Burner and measuring height

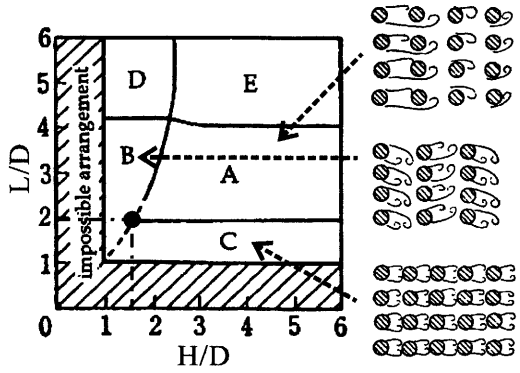

Fig. 7 Flow pattern map in tube-bank (uniform flow)[4]

perature distribution has significant influence on the NO_x formation. At the U-height, on the other hand, the transverse distribution of the gas temperature and concentrations is almost uniform. This suggests that the burner jet hardly reach there and hence the absence of the combustion reaction.

Second, on the (2)-line at the L-height, the gas temperature is at about 1 200 K, being relatively high in the transverse tube-to-tube region, and decreases to about 1 100 K in the wake regions. The CO-concentration shows thousands ppm in the region between tubes, and decreases to about hundreds ppm in the wake region. On the contrary, the NO_x-concentration shows about 20 ppm in the region between tubes, and increases to about 40 ppm in the wake region. The similar tendencies are observed at the M-height. In the transverse tube-to-tube region, the gas temperature and the CO-concentration are high, while the NO_x-concentration is low. In the wake region, on the contrary, the gas temperature and the CO-concentration are low and the NO_x-concentration is high.

Nishikawa et al.[4] carried out detailed investigation on Karman vortices in tube banks placed in a uniform flow, and proposed the flow pattern map shown in Fig. 7. The present case of $L/D = 1.97$ and $H/D = 1.57$ plotted by the solid dot is on the threshold boundary of the appearance of Karman vortices. Matsumoto et al.[5] carried out flow visualization experiment of the flow structure in the tube bank, having almost the same arrangement and pitches as the present tube bank, but impinged by a jet, and the Karman vortices were hardly observed in the wake region of the second row. These facts suggest the existence of the recirculation flow in the wake similar to the C-pattern in Fig. 7, less mixed with the main stream issued by the burner jet. It is thus expected that the mainstream retains high temperature due to the combustion reaction, while complete oxidization of CO takes place during the long residence time caused by the recirculation flow in the wake. Since the burning gas is exposed to the high temperature region over a long period, the NO_x-concentration becomes, on the contrary, high. At the U-height, both the gas temperature and gas concentrations show similar tendencies to those on the (1)-line at the U-height.

The distribution of gas temperature and gas concentrations on the (3a)-line at the L- and M-height show almost the same tendency as those on the (2)-line. However, the CO-concentration is not so high, and the NO_x-concentration is kept at relatively uniform distribution, compared with those on the (2)-line. The fluctuation in the O_2-concentration observed on the (2)-line becomes less significant on the (3a)-line. This may be due to the progress in the combustion reaction. At the U-height, the gas temperature is high but uniform between the transverse tube-to-tube regions, compared with that on the (2)-line. The gas concentrations are still uniform similarly to those on the (1)- and (2)-line at the U-height. The burner jet spreads and reaches this region, while the combustion reaction may not occur.

The measured results of the gas temperature and gas concentrations on the (3b)-, (4)- and (5)-line show almost the same tendency as those on the (3a)-line. The fluctuations in the transverse distribution become weak gradually with the flow. In these regions, the CO-concentration reduces to about several 10 ppm of the exhaust gas level.

On the (7)- to (11)-line, the gas concentrations show uniform distribution not only in the transverse direction but also in the longitudinal direction. On the other hand, the gas temperature is high in the transverse tube-to-tube region, while low in the wake region. This is mainly because of the heat absorption by the extended surface.

Summarized the above discussion, in the region from the burner down to the (5)-line at the L- and M-height, the combustion gas temperature and gas concentrations show finite amplitude fluctuations in both longitudinal and

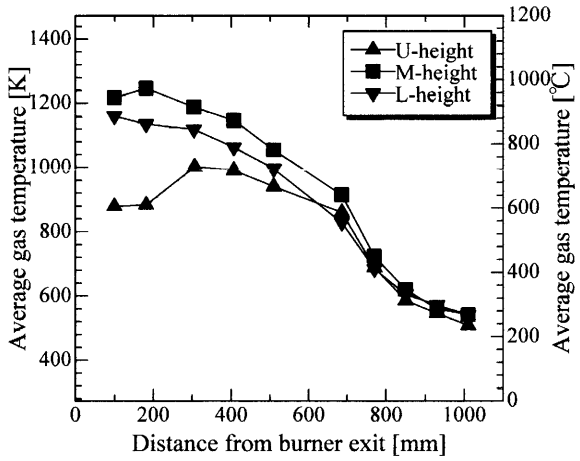

Fig. 8 Longitudinal distribution of average gas temperature

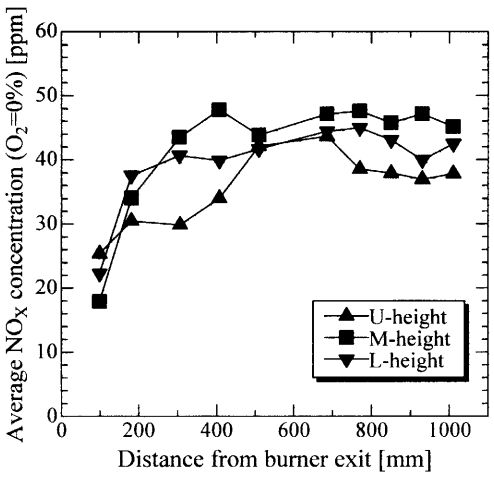

Fig. 9 Longitudinal distribution of average NO_x concentration (at 0% O_2)

transverse distribution. On the other hand at the U-height, the gas concentrations are rather uniform, while even a slight change is observed in the transverse distribution of the gas temperature. In other words, the combustion characteristics are controlled by the thermal-hydraulics in the region upstream the (5)-line in the present test boiler. To achieve further improvement for the low-NO_x combustion, it is essential to optimize the burner and the tube arrangement in this region.

5. Average Gas Temperature and Gas Concentrations

The distribution of gas temperature, the NO_x-concentration at 0% O_2 and the CO-concentration, averaged over the transverse wall-to-wall distance in the furnace, are plotted, respectively, in Figs. 8 to 10.

From the burner to the (5)-line (X = 0 to 509 mm), the average gas temperature at the L- and M-height decreases gradually with the gas stream. This means that the heat release rate by the combustion approximately balanced the heat absorption rate by the tube bank. The combustion reaction induces an increase, but limited to a low level, in the NO_x-concentration there, while a decrease in the CO-concentration is drastic. This is a typical feature of the JAFI combustor. The profiles of the temperature and NO_x-concentration at the U-height are different from those at the L- and M-height, but approach successively in accordance with the flow as is observed typically in the temperature distribution in Fig. 8.

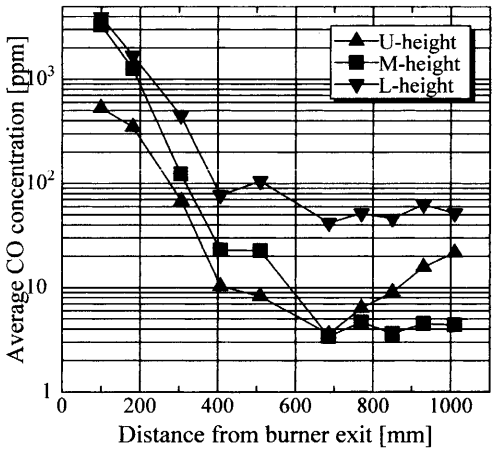

Fig. 10 Longitudinal distribution of average CO concentration

In the tube-bank downstream the (5)-line, the gas temperature decreases very rapidly, and the NO_x- and CO-concentration retain almost constant values. Thus the region is a heat absorbing zone without combustion reaction.

6. Heat Transfer Characteristics

The energy balance in the furnace was estimated based on the following assumptions:

(1) Gas and tube-wall temperatures in the furnace are represented by the measured values at the M-height.

(2) The combustion reaction is completed at the burner exit and the corresponding gas temperature is represented by the adiabatic flame temperature.

(3) The combustion gas velocity in the furnace is uniform along the transverse and vertical coordinates.

(4) The gas temperature drop in the flow direction is determined only by the heat absorption rate by the tube-bank.

6.1 Heat absorption by the tube-bank

As shown in Fig. 11, the furnace was subdivided in six sections, and the heat absorption rate across each section was estimated by Eq. (1).

$$Q_j = M \cdot c_p \cdot \Delta T \qquad (1)$$

where

Q_j : heat absorption rate in each section [W]

M : mass flow rate determined from the fuel and air flow rates at the burner entrance [kg/s]

c_p : specific heat of combustion gas [J/kgK]

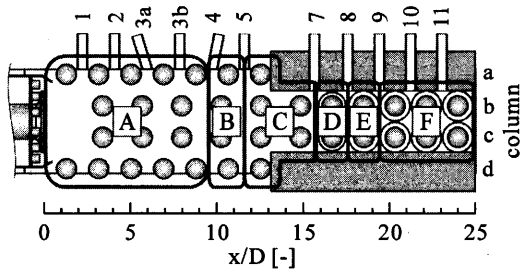

(a) Combustion subsections

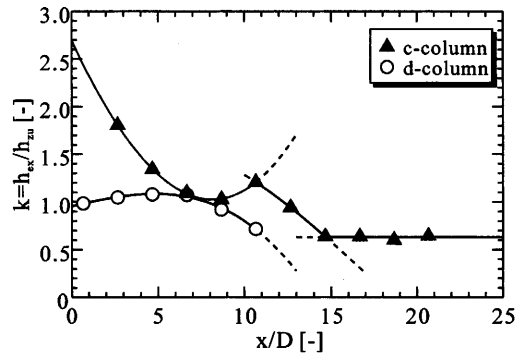

(b) Correction factors

Fig. 11 Heat balance estimation

ΔT : inlet-outlet temperature difference in each section [K]

Based on the assumption (2), the inlet temperature of the region A is given by Eq. (2)[6].

$$T_{bt} = \frac{0.97 \cdot H}{G_w \cdot c_{pb}} + T_0 \tag{2}$$

where

T_{bt} : adiabatic flame temperature [K]
H : heat release rate [W]
G_w : mass of wet burnt gas [kg/kg]
c_{pb} : average specific heat [J/kgK]
T_0 : reference (room) temperature [K]

6.2 Heat transfer by convection

The convective heat transfer in the tube-bank is estimated by Eq. (3).

$$Q_{con} = A \cdot h \cdot (T - T_w) \tag{3}$$

where

Q_{con} : heat absorption rate by convective heat transfer [W]
A : heat transfer area [m^2]
h : heat transfer coefficient [W/m^2K]
T : water-tube ambient temperature [K]
T_w : water-tube surface temperature [K]

Zukauskas[7] proposed an empirical formula of the heat transfer coefficient for an in-line tube-bank immersed in a uniform velocity profile, given by Eq. (4).

$$h_{zu} = 0.27 \cdot \frac{\lambda}{D} \cdot Re^{0.63} \cdot Pr^{0.36} \cdot \left(\frac{Pr}{Pr_w}\right)^{0.25} \tag{4}$$

where

h_{zu} : heat transfer coefficient of Zukasukas' equation [W/m^2K]
λ : thermal conductivity [W/mK]
D : outer diameter of water-tube [m]
Re : Reynolds number [-]
Pr : Prandtl number [-]
Pr_w : Prandtl number corresponding to the wall temperature [-]

On the other hand, Ozawa et al.[8] and Shintani[9] reported that Zukauskas' equation could not be applied to the tube-bank impinged by a burner jet. Therefore, h was determined by Eq. (5), i.e. modified Zukauskas' equation by Shintani's experimental results h_{ex}[9], where the correction factors k defined by Eq. (6) are shown in the lower column in Fig. 11.

$$h = 0.27 \cdot k \cdot \frac{\lambda}{D} \cdot \mathrm{Re}^{0.63} \cdot \mathrm{Pr}^{0.36} \cdot \left(\frac{\mathrm{Pr}}{\mathrm{Pr}_w}\right)^{0.25} \tag{5}$$

$$k = h_{ex}/h_{zu} \tag{6}$$

6.3 Heat transfer by radiation

The burning flame was non-luminous flame, and thus it seems reasonable to assume that the effect of luminous flame on the radiant heat transfer is negligible. Then only the radiations from CO_2 and H_2O were taken into account in the present estimation. These radiations are given by Eqs. (7) and (8), respectively, and Eq. (9)[10].

$$q_{CO_2} = \frac{1.436}{3\,600} \cdot S \cdot (P_{CO_2} \cdot s)^{1/3} \cdot \left\{\left(\frac{T}{100}\right)^{3.5} - \left(\frac{T_w}{100}\right)^{3.5}\right\} \tag{7}$$

$$q_{H_2O} = \frac{14.36}{3\,600} \cdot S^3 \cdot P_{H_2O}^{0.8} \cdot s^{0.6} \cdot \left\{\left(\frac{T}{100}\right)^{3} - \left(\frac{T_w}{100}\right)^{3}\right\} \tag{8}$$

where

q_{CO_2} : radiation of CO_2 [W/m^2]
q_{H_2O} : radiation of H_2O [W/m^2]
P_{CO_2} : partial pressure of CO_2 [Pa]
P_{H_2O} : partial pressure of H_2O [Pa]
ε_w : emissivity of water-tube surface [-]
S : $=\varepsilon_w/4.88$ [-]
s : gas reservoir thickness ($=\alpha \cdot a$) [m]
α : multiplier factor [-]
a : representative length [m]

$$Q_{rad} = (q_{CO_2} + q_{H_2O}) \cdot A \tag{9}$$

where Q_{rad}: heat absorption rate by radiation [W]. The emissivity ε_w(= 0.6) was a conventional value for a carbon steel used for boiler tubes.

6.4 Heat transfer characteristics

Table 3 shows the heat balance in each section estimated by the above-mentioned procedure. The sum of convective and radiant heat transfers in each respective section approximately agree with the heat absorption rate by Eq. (1).

Table 3 Estimated heat balance in the tube-nested combustor

Region (j)	Heat absorption rate by Eq.(1) Q_j [kW]	Heat transfer rate by convection Q_{con} [kW] (Q_{con}/Q_j [%])	Heat transfer rate by radiation Q_{rad} [kW] (Q_{rad}/Q_j [%])
A	138.7	100.8(72.6)	38.7(27.9)
B	23.4	16.8(71.8)	6.6(28.2)
C	34.3	28.5(83.1)	7.7(22.4)
D	45.2	30.9(68.4)	5.9(13.1)
E	23.4	17.2(73.5)	3.4(14.5)
F	19.3	23.1(ca. 100)	3.6(18.7)
Total	284.3	217.3(76.4)	65.9(23.2)

In the sections A and B, more than half of the total heat was absorbed. The region plays a very important role not only of the combustion but also of the heat exchange. Even though the combustion flame exists in those sections, the fraction of radiant heat transfer is rather low and the convective heat transfer dominates, i.e. more than 70% of the heat absorption rate, owing to the existence of tube-bank in this region and very high velocity of burning gas there.

In the subsequent sections C to F, being considered as the heat exchanger zone, heat absorption rate by radiation becomes rather low and the convective heat transfer is still dominant. In the whole furnace, the fraction of convective heat transfer reaches about 76% of the total absorption rate, which is a typical characteristics of the tube-nested combustor being different from traditional boilers.

7. Conclusion

Experimental investigation on the combustion characteristics was conducted by using 0.5 t/h test facility of the tube-nested combustor, and the distribution of temperature and gas concentrations was obtained. Such distribution verified the soundness of the design principles, and at the same time gave relevant information available for the R&D of the next generation tube-nested combustor.

Acknowledgements

Authors wish to express their sincere thanks to Messrs R. Yoshida, T. Kawae and N. Okuda. This experiments was supported by Hirakawa-Guidam Co. Ltd. This research was financially supported by the Kansai University Research Grants: Grant-in-Aid for Joint Research, 2001/2002.

References

(1) Ishigai, S., Kobayashi, H., Kurimoto, K., Hasebe, H. and Okada, H., Development of New Type Boilers with JAFI Combustors, Proc. ICOPE-93, Tokyo, Vol.2 (1993), pp.343–348.

(2) Ueda, Y., Ishigai, S., Ozawa, M., Kurimoto, K., Hasebe, H., Okada, H. and Kaminashi, A., Experimental Study of a New Type Boiler with Tube-Nested Combustor, Proc. ICOPE-95, Shanghai, Vol.1 (1995), pp.357–362.

(3) United States Patent, Patent No.5020479, Date of Patent Jun, 4, (1991).

(4) Nishikawa, E., General Planning of the Boiler Gas-Side Heat Transfer Surface, edited by Ishigai, S., Steam Power Engineering, Chap.5, (1999), Cambridge University Press, New York.

(5) Matsumoto, R., Shintani, Y., Okada, M., Imahori, K., Ohnishi, T., Ishihara, I. and Ozawa, M., Flow Pattern in a Simulated Tube-Nested Combustor, J. of the Visualization Society of Japan, (in Japanese), Vol.22 (2002), pp.15–22.

(6) Mizutani, Y., Combustion Engineering, Second edition, (in Japanese), (1989), Morikita Publishing, Tokyo.

(7) Zukauskas, A. and Uliskas, R., Heat Transfer in Tube Banks in Crossflow, (1988), Hemishpere, New York.

(8) Ozawa, M., Ueda, Y., Hasegawa, M. and Kobayashi, H., Convective Heat Transfer in a Tube Bank Impinged by a Round Jet, Proc. ICOPE-93, Tokyo, Vol.1 (1993), pp. 197–202.

(9) Shintani, Y., Characteristics of Combustion and Heat Transfer in a Tube-Nested Combustor, (in Japanese), (2002), Mater Thesis, Kansai University, Osaka.

(10) Honda, N., New Combustion Engineering of the Environmental Area, (in Japanese), (1999), Fuji Techno-System, Tokyo.